2D Metal-Organic Framework Derived Ultra-Thin Nitrogen-doped Oxygen Rich Porous Carbon Nanosheets for Zinc-Ion Hybrid Supercapacitors

Yu Han[a,c], Chiyu Zhang[a], Kai-Jie Chen[a,*], and Teng Wang[a,b,c*]

[a]*Key Laboratory of Special Functional and Smart Polymer Materials of Ministry of Industry and Information Technology, Xi'an Key Laboratory of Functional Organic Porous Materials, School of Chemistry and Chemical Engineering, Northwestern Polytechnical University, 127 West Youyi Road, Xi'an, Shaanxi 710072, PR China. Email: ckjiscon@nwpu.edu.cn; wangt42@nwpu.edu.cn.*

[b]*National and Local Joint Engineering Laboratory for Slag Comprehensive Utilization and Environmental Technology, School of Materials Science and Engineering, Shaanxi University of Technology, Hanzhong 723000, Shaanxi, China.*

[c]*Key laboratory of Flexible Electronics of Zhejiang Province, Ningbo Institute of Northwestern Polytechnical University, 218 Qingyi Road, Ningbo, 315103, PR China.*

Experimental Section

***Chemicals**:* Benzimidazole (98%), 1-hexanol (98%), n-heptane (99%), zinc acetate dihydrate ($Zn(CH_3COO)_2 \cdot 2H_2O$, 98%), zinc sulphate ($ZnSO_4 \cdot 7H_2O$, AR) and zinc trifluoromethanesulfonate ($Zn(CF_3SO_3)_2$, AR) were purchased from Aladdin. Cetyltrimethylammonium bromide (CTAB, $C_{19}H_{42}NBr$, 99%) was purchased from Macklin. Potassium hydroxide (KOH, 95%) was purchased from 3A Chem. Deionized water with a resistivity of 18.25 MΩ cm was used. Carbon fiber clothes were provided by ElectroChem Inc (USA). Zinc plates were purchased from Corud. All the chemicals were used without further purification.

Synthesis of Zn(bim)(OAc): Zn(bim)(OAc) was synthesized according to a previously reported proced. with some modifications.[1] 5.4 ml benzimidazole solution (0.6 M in 1-hexanol) and 2.7 ml

zinc acetate dihydrate solution (1.2 M in water) were added to a suspension containing 3.645 g CTAB and 200 ml of the mixt. of n-heptane and 1-hexanol (V: V=9:1) under stirring. The reaction solution was stirred vigorously at room temperat. for 10 min and then heated to 60 °C for a further 20 hours' reaction to achieve Zn(bim)(OAc). Subsequently, the solution was centrifuged at 8000 r for 8 minutes, washed three times with n-heptane, and dried in an oven at 75 °C for 24 hours to obtain Zn(bim)(OAc).

Synthesis of NOCNS: Zn(bim)(OAc) was put into a tube furnace under an Ar flow for 2 h to exclude air, and then carbonized at different temperat.s (600 °C, 700 °C, 800 °C, 900 °C, and 1000 °C) for 2 h with a heating rate of 5 °C min^{-1} to produce NOCNS-T (T = 600, 700, 800, 900, and 1000, respectively, **Table S1**).

Synthesis of A-NOCNS: The NOCNS was thoroughly mixed with KOH activation reagent at a NOCNS/KOH weight ratio of 1:4. Subsequently, the mixt. was transferred into a tube furnace and activated under an Ar flow at different temperat.s (300 °C, 400 °C, and 500 °C) for 30 minutes with a heating rate of 5 °C min^{-1}. After activation, the yielded powders were washed by dilute HCl aqueous solution and distilled water thoroughly and finally dried at 80 °C overnight to gain MOF-derived carbon (classified as A-NOCNS-T and the name rules are shown in **Table S1**).

Characterizations*:* XRD patterns of as-made samples were collected using a powder X-ray diffractometer (XRD, Rigaku Mini Flex 600 with Cu Kα radiation). Raman spectra were recorded using a Raman spectrometer (WITec Alpha 300R). Morphological feat.s of the samples were characterized by scanning electron microscope (SEM, Verios G4, FEI), transmission Electron Microscope (TEM, FEI Talos F200X), and atomic Force Microscope (AFM, Bruker). BET and the pore struct. of the samples were characterized by the N_2 gas sorption test (Micromeritics 3Flex). The compositions of the samples were investigated using energy dispersive spectroscopy (EDS). The

surface compositions of the samples were analyzed by X-ray photoelectron spectroscopy (XPS, Thermo Fisher Scientific KAlpha). WCA meas.ments were characterized by a contact angle meter (Dong Guan Precise Test Equipment Co., Ltd).

Electrochemical Performance Measurements: The cathode electrodes are prepared as follows: Mix 80wt% activated carbon, 10wt% carbon black, and 10wt% polyvinylidene difluoride (PVDF) binder in n-methyl-2-prrodilinone (NMP) solvent to form a slurry, which was painted onto carbon cloth current collector and dried at 70 °C in a vacuum oven for 10 h. The active mass loading of the electrodes is ~1.0 mg cm^{-2}. The electrochemical performance of the electrodes was meas.d via a three-electrode system and all the data were collected by an electrochemical workstation (VSP, BioLogic). For the 3-electrode test set, the as-synthesized cathode electrodes as the working electrode, standard Hg/HgO electrode as the reference electrode, and Pt foil (1*2 cm^2) as the counter electrode were employed. The cycling stability tests of the as-synthesized materials were tested using a program-control automatic system (NEWARE-CT-4008). The accuracy of the electronic balance is d=0.01 mg (METTLER TOLEDO-ME55)

Assembly of ZIHSCs: The as-prepared cathode electrodes, Zn foil anode (1*1 cm^2), and neutral electrolytes (2M $Zn(CH_3COO)_2$, 2M $ZnSO_4$, and 2M $Zn(CF_3SO_3)_2$) were employed to assemble the ZIHSCs.

The specific capacity (Q_s, mAh g^{-1}), energy density (E, Wh kg^{-1}), and power density (P, W kg^{-1}) of ZIHSCs were calculated based on equations (1-3):

$$Q_S = \frac{I}{m} \times \frac{\Delta t}{3.6} \tag{1}$$

$$E = \frac{I \int_{t_i}^{t_f} V_s dt}{3.6m} \tag{2}$$

$$P = \frac{3600 \times E}{\Delta t} \tag{3}$$

I (A) is the corresponding current. m (g) is the mass of positive materials. V_s (V) is the operating voltage. t_i and t_f are the initial and final values of discharge time t (s).

Table S1. Name rules for the as-obtained carbonized materials.

Number	Temperat. (°C)	Name
1	600 °C	NOCNS-600
2	700 °C	NOCNS-700
3	800 °C	NOCNS-800 (NOCNS)#
4	900 °C	NOCNS-900
5	1000 °C	NOCNS-1000
6	800 °C, 300 °C	A-NOCNS-300
7	800 °C, 400 °C	A-NOCNS-400 (A-NOCNS)#
8	800 °C, 500 °C	A-NOCNS-300

For convenience, NOCNS-800 is abbreviated as NOCNS, and A-NOCNS-400 is abbreviated as A-NOCNS.

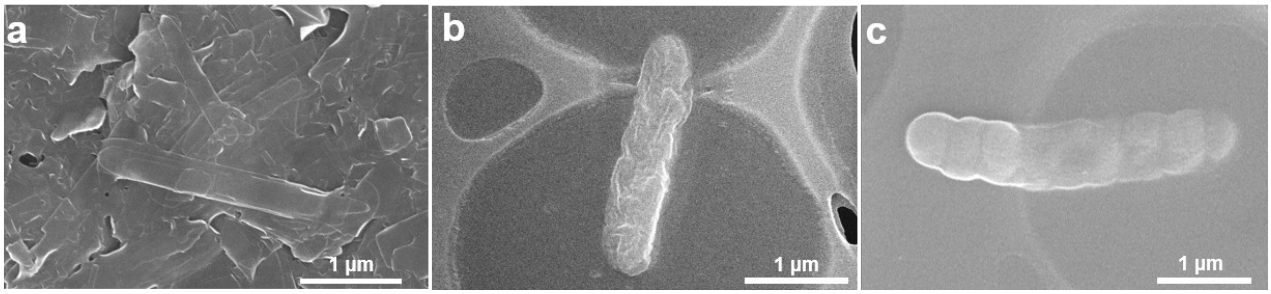

Fig. S1. SEM images of (a) Zn(bim)(OAc), (b) NOCNS, and (c) A-NOCNS.

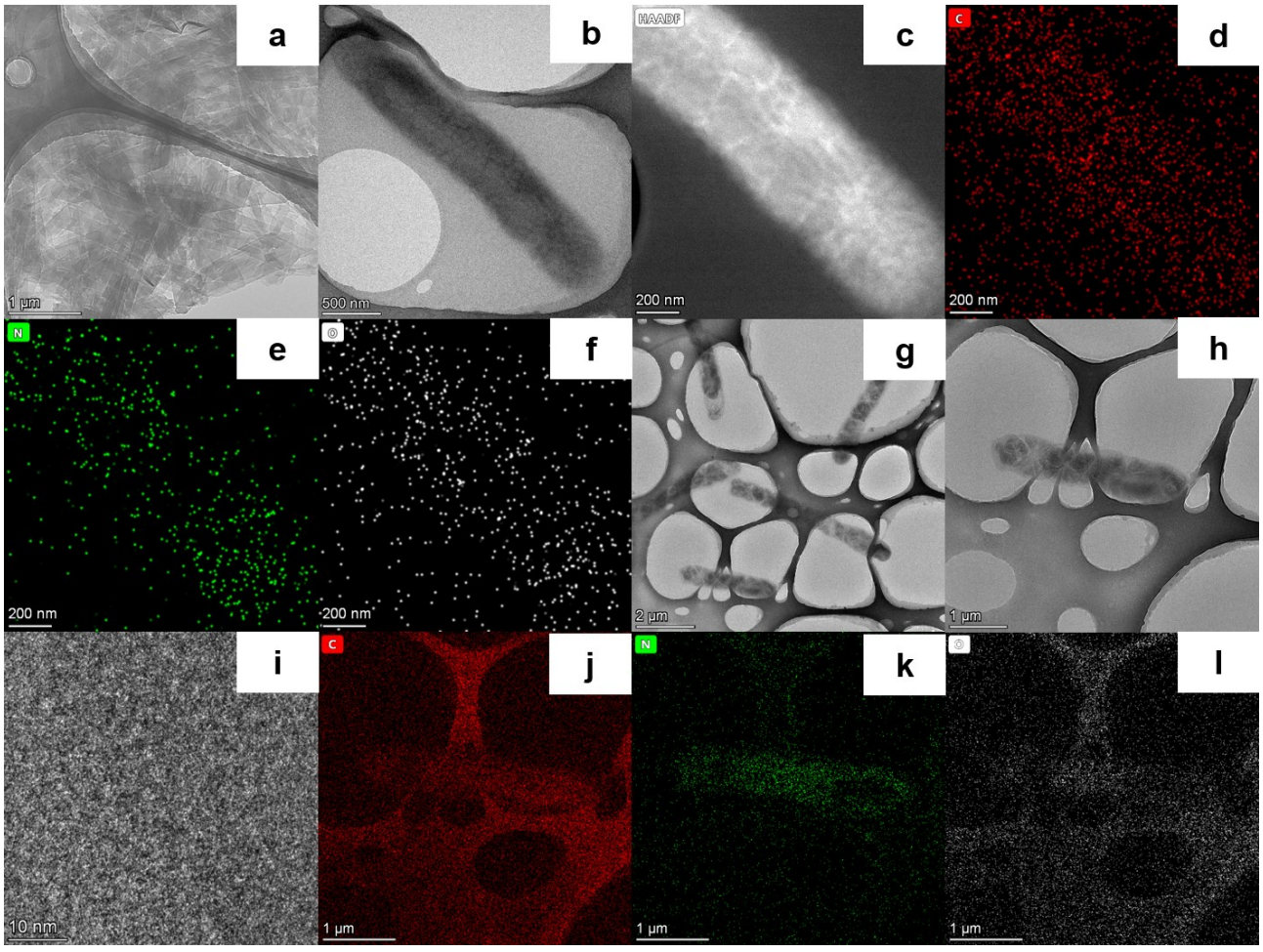

Fig. S2. TEM images of (a) Zn(bim)(Oac) and (b) NOCNS; (c) HAADF image of NOCNS; (d-f) TEM elemental mapping images of NOCNS; (g-i) TEM images of A-NOCNS; (j-l) TEM elemental mapping images of A-NOCNS.

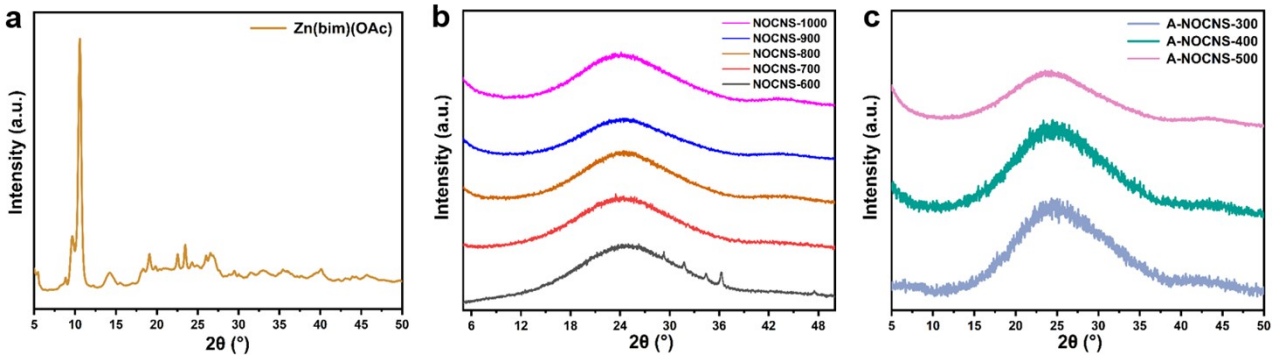

Fig. S3. XRD patterns: (a) Zn(bim)(OAc); (b) NOCNS-T (T= 600, 700, 800, 900, 1000); (c) A-NOCNS-T (T= 300, 400, 500).

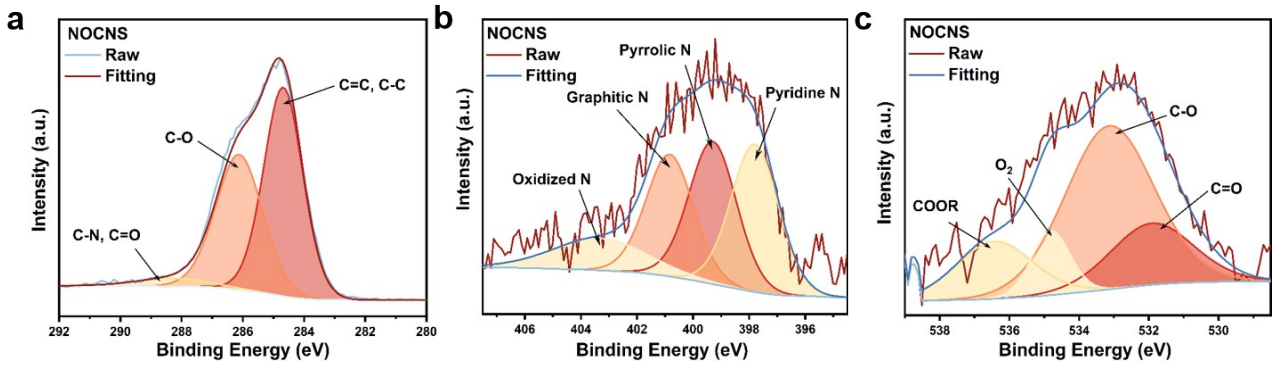

Fig. S4. XPS spectra of NOCNS: (a) C 1s, (b) N 1s, and (c) O 1s.

Table S2. Porosity characteristics of the as-obtained A-NOCNS and NOCNS.

Sample	V_t ($cm^3\ g^{-1}$)	S_{BET} ($m^2\ g^{-1}$)	$S_{micropore}$ ($m^2\ g^{-1}$)	$S_{micropore}/S_{BET}$ (%)
NOCNS	0.52	396.12	147.88	37.33
A-NOCNS	0.42	528.38	279.87	52.97

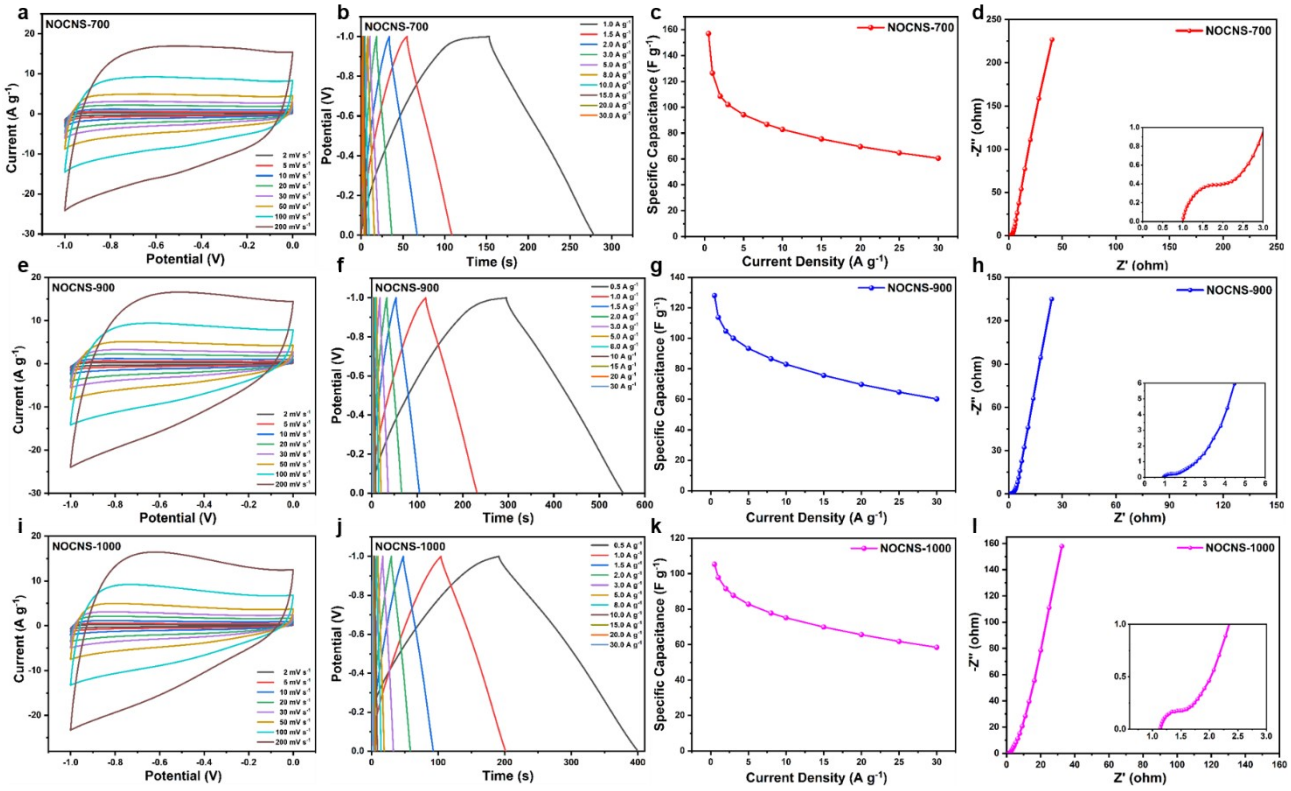

Fig. S5. (a-d) Electrochemical performance of NOCNS-700: (a) CV curves, (b) GCD curves, (c) Calculated specific capacitance results, and (d) EIS spectra; (e-h) Electrochemical performance of NOCNS-900: (e) CV curves, (f) GCD curves, (g) Calculated specific capacitance results, and (h) EIS spectra; (i-l) Electrochemical performance of NOCNS-1000: (i) CV curves, (j) GCD curves, (k) Calculated specific capacitance results, and (l) EIS spectra.

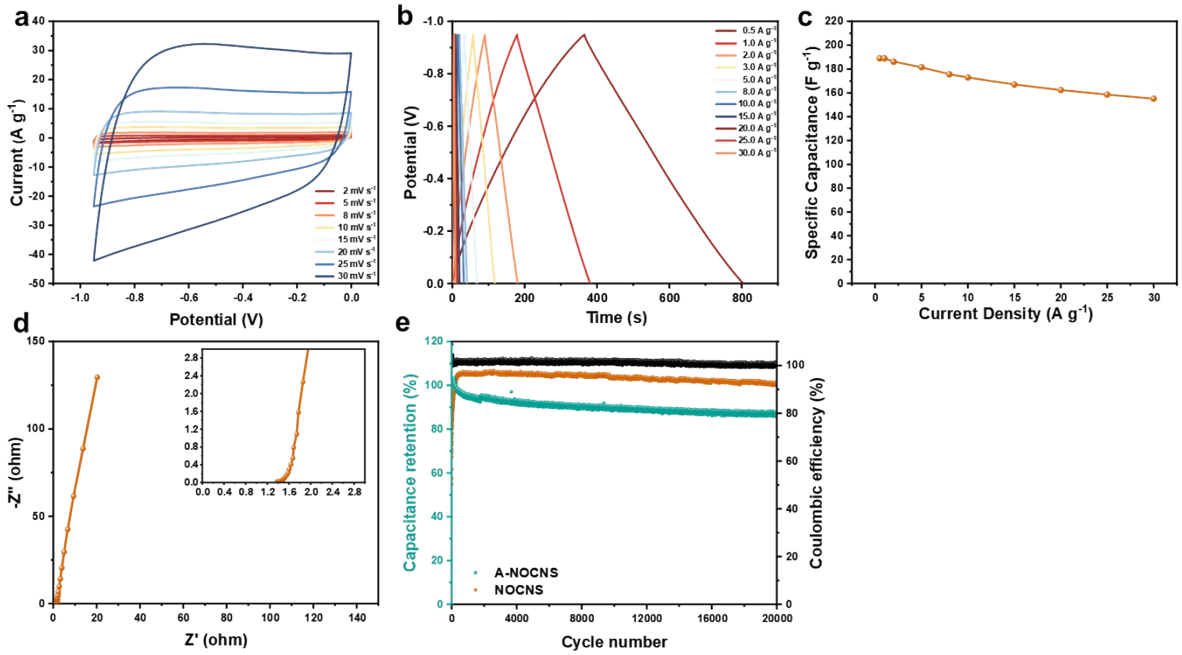

Fig. S6. Electrochemical performance of NOCNS (NOCNS-800): (a) CV curves; (b) GCD curves; (c) Calculated specific capacitance results; (d) EIS spectra. (e) Long-term cycling performance for NOCNS and A-NOCNS at the current density of 10 A g^{-1}.

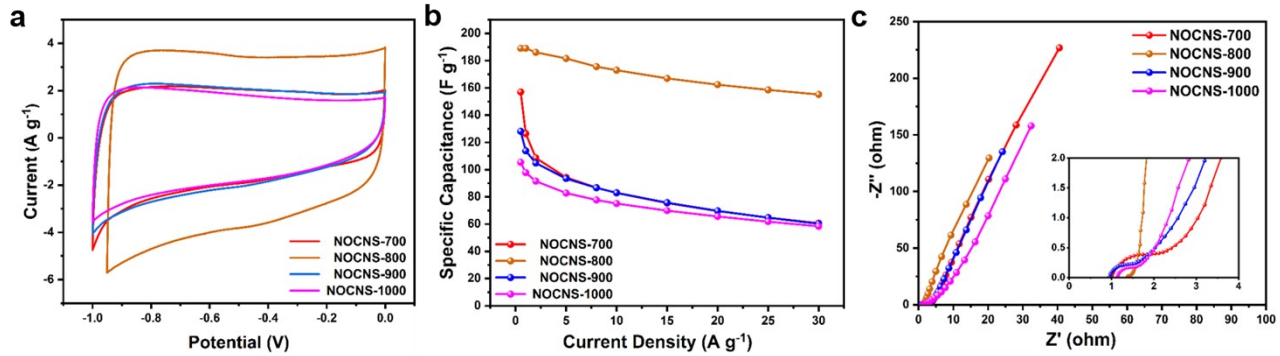

Fig. S7. Comparison of (a) CV curves at a scan rate of 20 mV s^{-1} in 2M KOH, (b) Calculated specific capacitance at different current densities, and (c) EIS spectra of NOCNS-T samples.

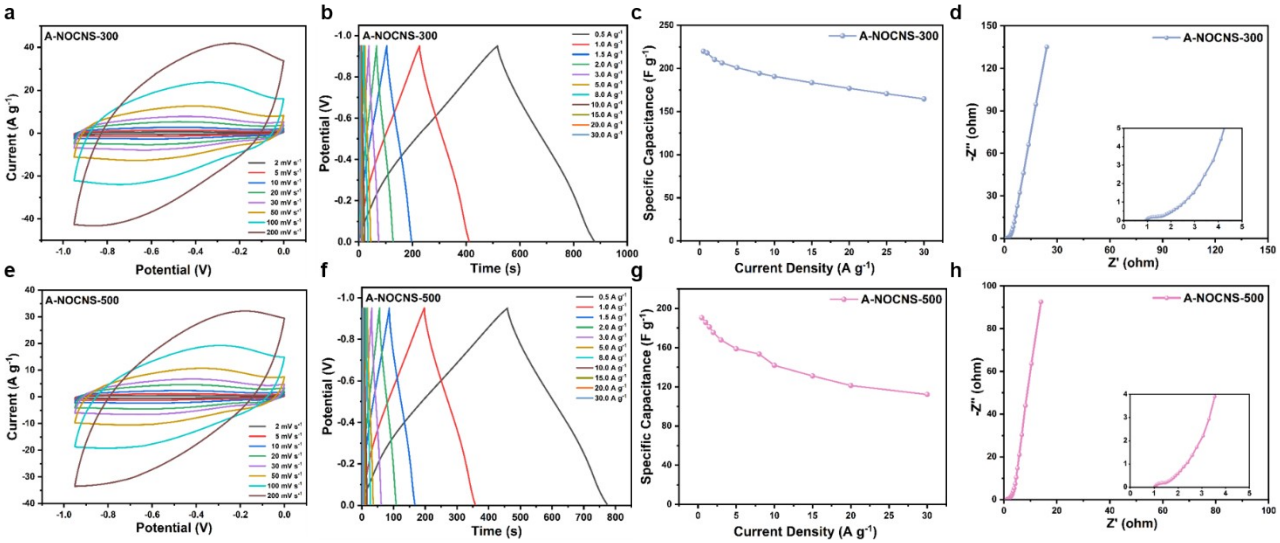

Fig. S8. (a-d) Electrochemical properties of A-NOCNS-300: (a) CV curves at different scan rates, (b) GCD curves, (c) Calculated specific capacitance at different current densities, and (d) EIS spectra. (e-h) Electrochemical properties of A-NOCNS-500: (e) CV curves at different scan rates, (f) GCD curves, (g) Calculated specific capacitance at different current densities, and (h) EIS spectra.

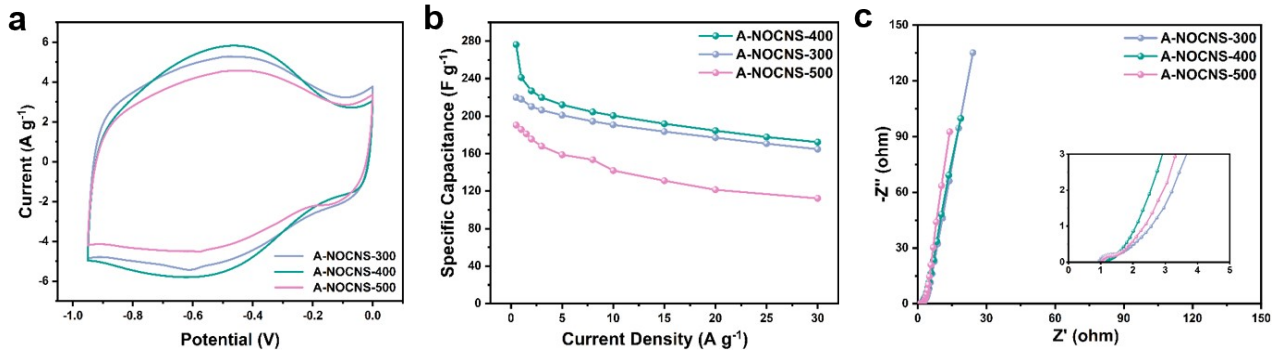

Fig. S9. Comparison of (a) CV plots at 20 mV s^{-1}, (b) Specific capacitance results, and (c) EIS spectra of A-NOCNSs in different activation temperat.s (A-NOCNS-300, A-NOCNS-400, and A-NOCNS-500).

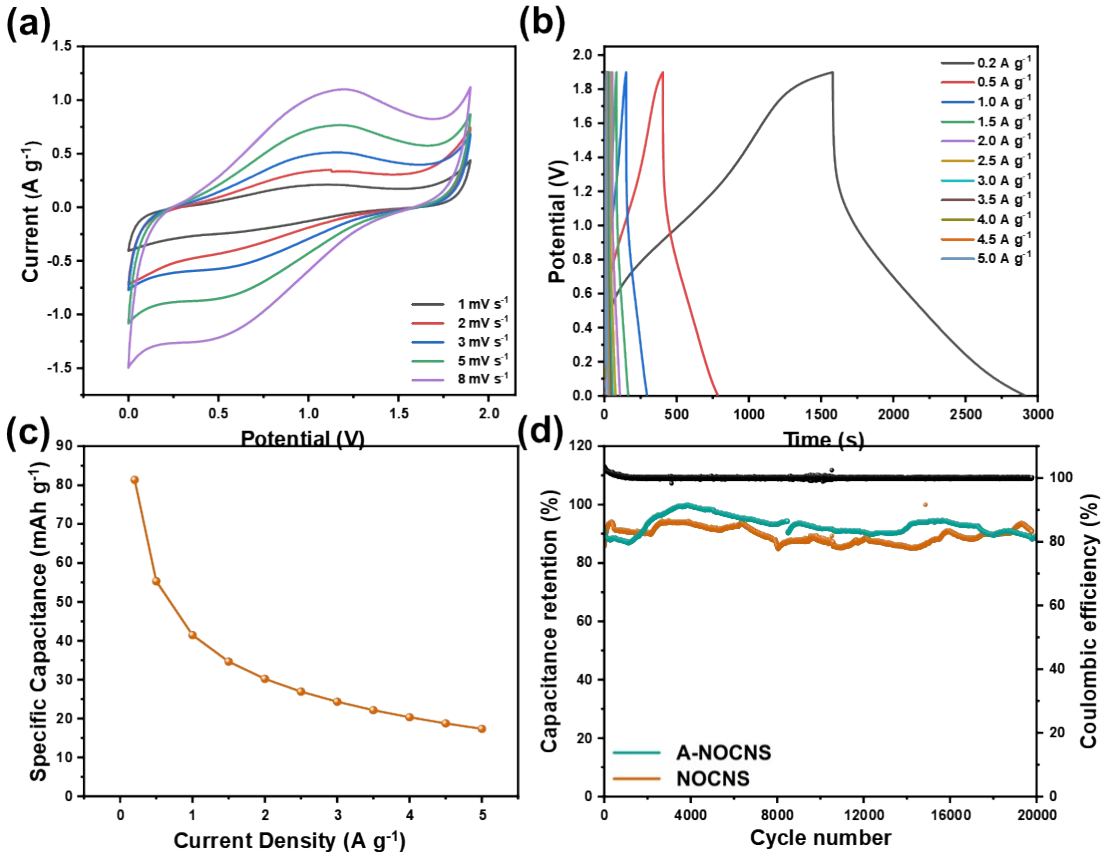

Fig. S10. The electrochemical properties of ZIHSCs based on NOCNS in $ZnSO_4$ electrolyte: (a) CV curves at different scan rates; (b) GCD curves at various current densities; (c) Specific capacity at various current densities. (d) Cycling stability based on A-NOCNS and NOCNS for 20000 cycles at 10 A g^{-1}.

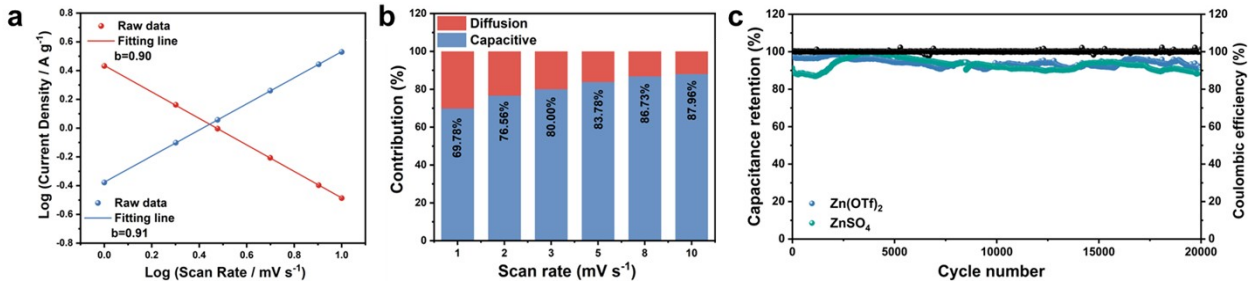

Fig. S11. (a) The b-value obtained from the linear relationship between log(i) and log(v). (b) The percentage of capacitive contributions at different scan rates of A-NOCNS//$Zn(CF_3SO_3)_2$//Zn ZIHSC. (c) Cycling stability for A-NOCNS in $ZnSO_4$ and $Zn(CF_3SO_3)_2$ electrolyte for 20000 cycles at 10 A g^{-1}.

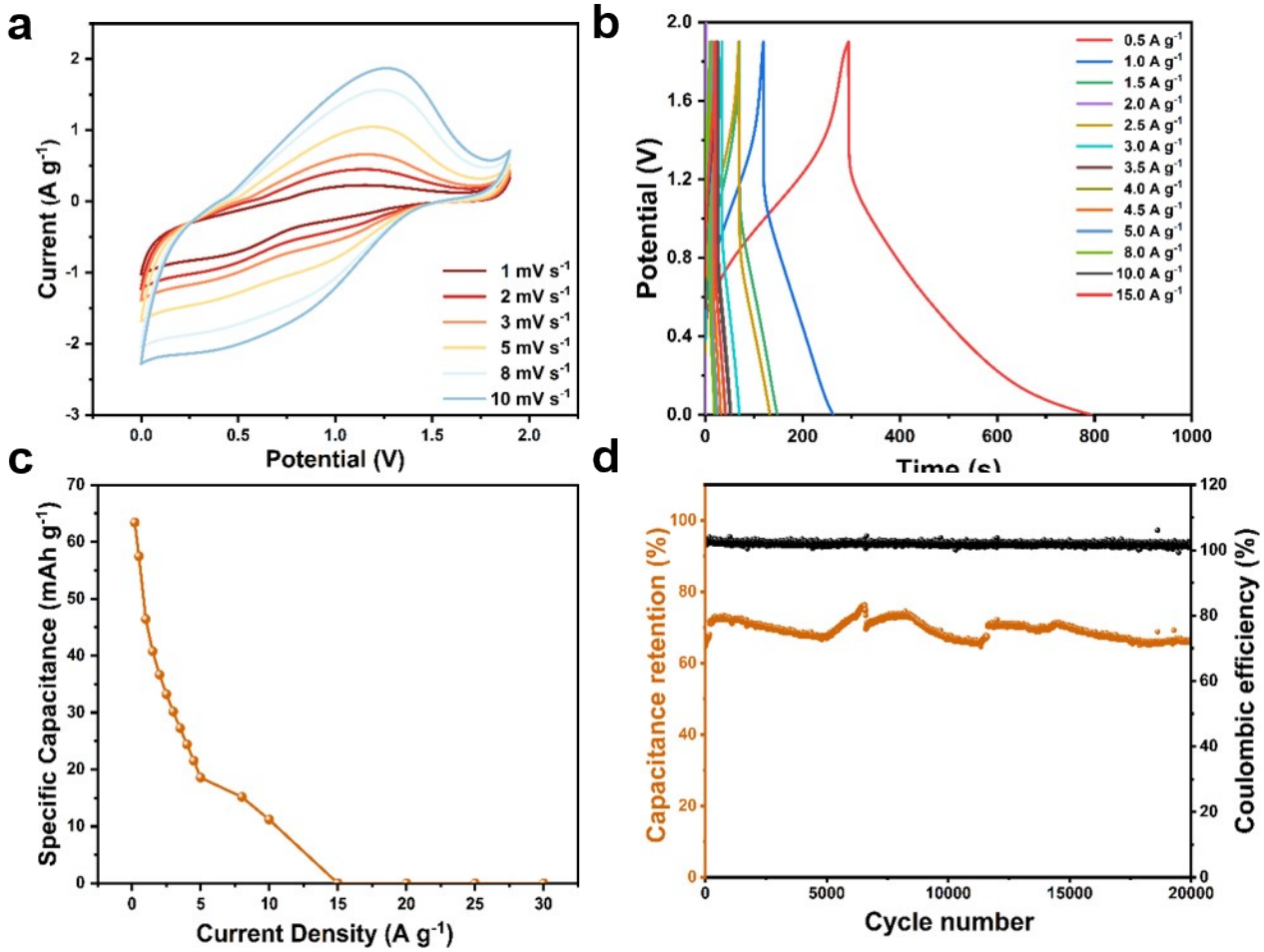

Fig. S12. The electrochemical properties of ZIHSCs based on A-NOCNS in $Zn(CH_3COO)_2$ electrolyte: (a) CV curves at different scan rates; (b) GCD curves at various current densities; (c) Specific capacity at various current densities; (d) Cycling stability for 20000 cycles at 1 A g^{-1}.

Table S3. Comparison of electrochemical properties of ZIHSCs assembled by diverse carbon-based cathodes.

Materials	Electrolyte	Potential (V)	Specific capacity (mAh g^{-1})/ Current density (A g^{-1})	Capacity retention (%)/ Cycle number (n)	Capacity retention (%)/ Current density range (A g^{-1})	Energy density / Wh kg^{-1}	Power density / kW kg^{-1}	Ref.
CPMD	3 M $ZnSO_4$	0-1.8	167.5 / 0.1	92.2 / 10000	44.8%/ 0.1-20	150.3	10.3	2
ZDC	2 M $ZnSO_4$	0.2-1.8	151.5 / 0.5	75 / 20000	37.1%/ 0.5-20	121.2	16	3
WC-6ZnN-12U	2 M $ZnSO_4$	0.2-1.8	111 / 0.1	92.7 / 50000	57.6%/ 0.1-3	109.5	6.75	4
PCNF-4	1 M $ZnSO_4$	0-1.7	177.7 / 0.5	~90 / 10000	/	142.2	15.39	5
LHPC-900	1 M $ZnSO_4$	0.2-1.8	132.4 / 0.1	97 / 10000	33.6%/ 0.1-20	135	10.2	6
NPC	1 M $ZnSO_4$	0-1.8	136.2 / 0.3	98.9 / 60000	50.8%/ 0.3-15	122.58	12.8	7
2DPC90	2 M $ZnSO_4$	0.2-1.8	198.4 / 0.2	~100 / 10000	57.2%/ 0.2-20	199.4	18.9	8
C-0.6	2 M $ZnSO_4$	0.2-1.8	181.67 / 0.05	91.25 / 40000	38.5%/ 0.05-20	145.2	14.5	9
GRPC-A13	2 M $ZnSO_4$	0.2-1.8	177 / 0.5	~83 / 20000	20.3%/ 0.5-10	116	8	10
MEHC-3	2 M $ZnSO_4$	0.2-1.8	132.9 / 0.2	94.7 / 20000	77.7%/ 0.5-5	106.4	40	11
AC	2 M $ZnSO_4$	0.2-1.8	121 / 0.1	91.0 / 10000	33.9%/ 0.1-20	84	14.9	12
AC	2 M $ZnSO_4$	0.2-1.8	132 / 0.1	72 / 20000	11.4%/ 0.1-16	140.8	2.85	13
O-riched PC	1 M $ZnSO_4$	0.2-1.8	132.7 / 0.2	87.6 / 10000	41.1%/ 0.2-4	82.4	3.76	14
N-HPC	2 M $ZnSO_4$	0.2-1.8	136.8 / 0.1	90.9 / 5000	48.6%/ 0.1-10	191	3.6	15
Graphene oxide film	2 M $ZnSO_4$	0.2-1.8	99.3 / 0.2	~90 / 10000	60.4%/ 0.2-10	76.2	3.54	16
MDPC-2	2 M $Zn(CF_3SO_3)_2$	0-1.8	161.7 / 0.5	96.5 / 10000	45.5%/ 0.5-50	145.5	45	17
$NPFC_{700}$	2 M $Zn(CF_3SO_3)_2$	0.2-1.8	163.6 / 0.1	~99 / 10000	57.9% / 0.1-20	60.1	35.9	18
PZC-A750	1 M $Zn(CF_3SO_3)_2$	0.2-1.8	124 / 0.25	~100 / 10000	65.9% / 0.25-20	107.3	16.65	19
AC	1 M $Zn(CF_3SO_3)_2$	0-1.8	94.4 / 0.1	~91 / 20000	~86% / 0.1-2	52.7	3.02	20
aMEGO	3 M $Zn(CF_3SO_3)_2$	0-1.9	110.83 / 0.1	93 / 80000	~47.6% / 0.1-20	106.3	31.4	21
PSC-A600	1 M $Zn(CF_3SO_3)_2$	0.2-1.8	183.7 / 0.2	92.2 / 10000	44.5% / 0.2-20	147.0	15.7	22
HPC-600	1 M $Zn(CF_3SO_3)_2$	0.2-1.8	169.4 / 0.1	93.1 / 60000	57.6% / 0.1-20	125.1	16.1	23
HPAC	3 M $Zn(CF_3SO_3)_2$	0-1.8	172.7 / 0.1	70 / 18000	69.1% / 0.1-20	117	11.4	24
PCC-3	1 M $Zn(CF_3SO_3)_2$	0.2-1.8	153.33 / 0.5	99 / 10000	66.7% / 0.5-20	119.0	13.24	25

A-NOCNS	2 M $ZnSO_4$	0-1.9	141.19 / 0.2	88.97 / 20000	49.9%/ 0.2-5	134.14	5.36	This work
	2 M $Zn(CF_3SO_3)_2$	0-1.9	176.48 / 0.2	90.23 / 20000	34.9%/ 0.2-30	162.88	28.43	

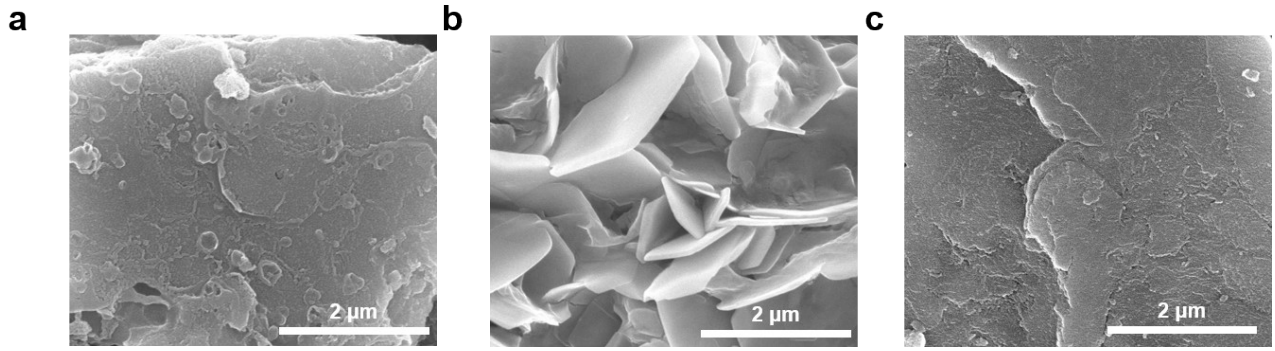

Fig. S13. (a-c) SEM images of A-NOCNS at different charge/discharge states in $Zn(CF_3SO_3)_2$.

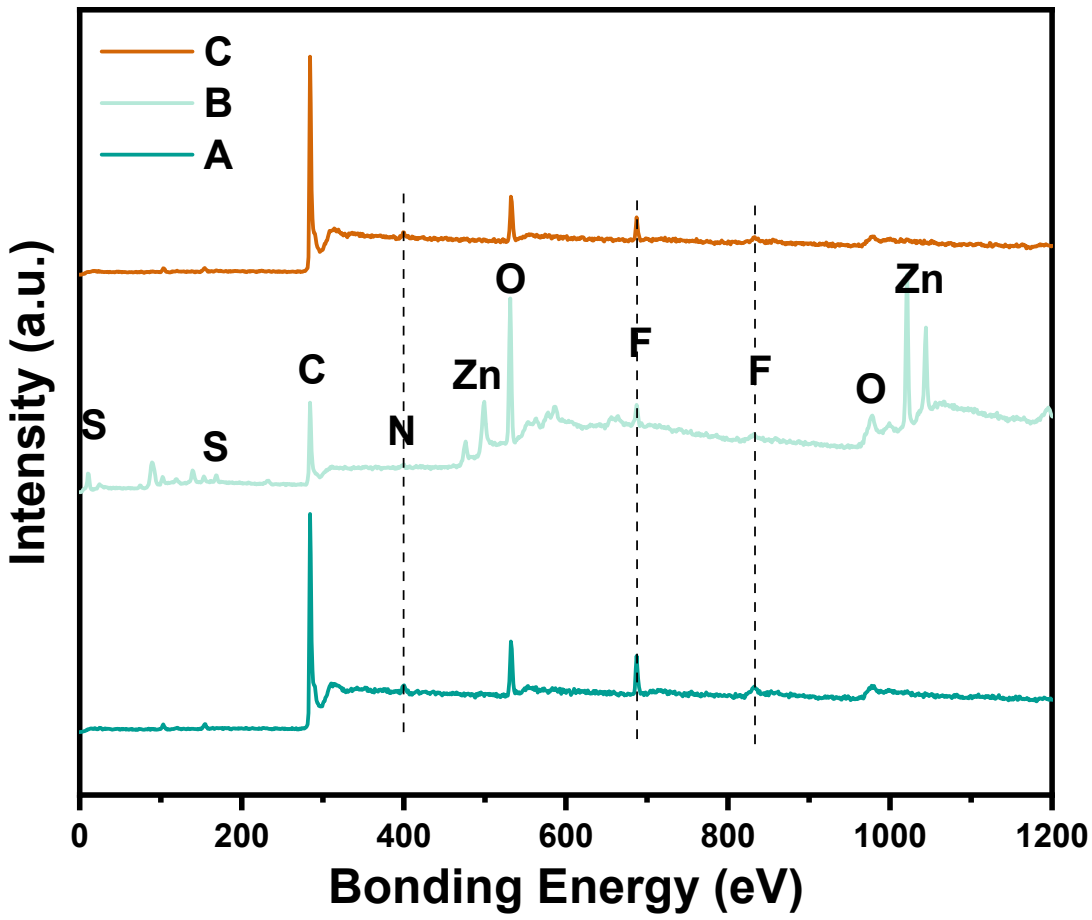

Fig. S14. XPS survey spectra of A-NOCNS at different charge/discharge states in $Zn(CF_3SO_3)_2$.

Table S4. The content of different coordinated C groups in the high resolution XPS spectra of C 1s in the A-NOCNS cathode of the corresponding ZIHSC at different charge/discharge states.

Element	Valence state	$Zn(CF_3SO_3)_2$		$ZnSO_4$	
		Binding energy (eV)	Content (%)	Binding energy (eV)	Content (%)
A	sp^2C	284.8	61.08	284.8	65.41
	C-O-H	286.0	26.85	285.9	24.61
	C-O-Zn	287.9	5.20	287.9	4.35
	C=O-O	290.8	6.86	290.9	5.63
B	sp^2C	284.7	64.39	284.8	63.13
	C-O-H	285.9	20.99	286.2	12.62
	C-O-Zn	287.8	9.09	287.8	7.05
	C=O-O	290.8	5.53	290.9	4.36
C	sp^2C	284.7	62.35	284.8	52.61
	C-O-H	285.9	26.98	286.1	31.38
	C-O-Zn	287.9	4.37	288.1	5.28
	C=O-O	290.7	6.29	290.8	9.75

Reference

1 F. Xue, P. Kumar, W. Xu, K. A. Mkhoyan, M. Tsapatsis, *Chem. Mater.* 2017, **30**, 69-73.

2 J. Li, S. Zhang, Y. Hua, Y. Lin, X. Wen, E. Mijowska, T. Tang, X. Chen, R. S. Ruoff, *Green Energy & Environ.* 2024, **9**, 1138-1150.

3 Y. Wei, X. Chen, G. Gao, D. Shen, H. Rong, Q. Liu, *Ionics* 2022, **28**, 3477-3488.

4 G. Lou, G. Pei, Y. Wu, Y. Lu, Y. Wu, X. Zhu, Y. Pang, Z. Shen, Q. Wu, S. Fu, H. Chen, *Chem. Eng. J.* 2021, **413**, 127502.

5 Z. Pan, Z. Lu, L. Xu, D. Wang, *Appl. Surf. Sci.* 2020, **510**, 145384.

6 L. Zhao, W. Jian, X. Zhang, F. Wen, J. Zhu, S. Huang, J. Yin, K. Lu, M. Zhou, W. Zhang, X. Qiu, *J. Energy Storage* 2022, **53**, 105095.

7 X. Shi, H. Zhang, S. Zeng, J. Wang, X. Cao, X. Liu, X. Lu, *ACS Mater. Lett.* 2021, **3**, 1291-1299.

8 H. Liu, S. Li, X. Huang, W. Chen, M. Xu, Y. Ren, R. Zhang, Z. Miao, J. Zhu, *Mater. Today Chem.* 2023, **29**, 101476.

9 X. Wei, B. Qiu, H. Tian, Y. Lv, W. Zhang, Q. Qin, Z. Liu, F. Wei, *Appl. Surf. Sci.* 2023, **615**, 156280.

10 L. Yao, J. Jiang, H. Peng, H. Yang, S. Liu, X. Wen, P. Cai, Y. Zou, H. Zhang, F. Xu, L. Sun, X. Lu, *J. Energy Storage* 2023, **58**, 106378.

11 D. Wang, Z. Pan, G. Chen, Z. Lu, *Electrochim. Acta* 2021, **379**, 138170.

12 L. Dong, X. Ma, Y. Li, L. Zhao, W. Liu, J. Cheng, C. Xu, B. Li, Q.-H. Yang, F. Kang, *Energy Storage Mater.* 2018, **13**, 96-102.

13 Z. Wang, J. Huang, Z. Guo, X. Dong, Y. Liu, Y. Wang, Y. Xia, *Joule* 2019, **3**, 1289-1300.

14 Y. Zheng, W. Zhao, D. Jia, Y. Liu, L. Cui, D. Wei, R. Zheng, J. Liu, *Chem. Eng. J.* 2020, **387**, 124161.

15 P. Liu, Y. Gao, Y. Tan, W. Liu, Y. Huang, J. Yan, K. Liu, *Nano Research* 2019, **12**, 2835-2841.

16 Y. Zhu, X. Ye, H. Jiang, J. Xia, Z. Yue, L. Wang, Z. Wan, C. Jia, X. Yao, *J. Power Sources* 2020, **453**, 227851.

17 H. Li, Q. Liao, Y. Liu, Y. Li, X. Niu, D. Zhang, K. Wang, *Small* 2023, **20**, 2307184.

18 F. Wei, Y. Wei, J. Wang, M. Han, Y. Lv, *Chem. Eng. J.* 2022, **450**, 137919.

19 X. Zhu, F. Guo, Q. Yang, H. Mi, C. Yang, J. Qiu, *J. Power Sources* 2021, **506**, 230224.

20 H. Wang, M. Wang, Y. Tang, *Energy Storage Mater.* 2018, **13**, 1-7.

21 S. Wu, Y. Chen, T. Jiao, J. Zhou, J. Cheng, B. Liu, S. Yang, K. Zhang, W. Zhang, *Adv. Energy Mater.* 2019, **9**, 1902915.

22 Z. Li, D. Chen, Y. An, C. Chen, L. Wu, Z. Chen, Y. Sun, X. Zhang, *Energy Storage Mater.* 2020, **28**, 307-314.

23 L. Wang, M. Huang, J. Huang, X. Tang, L. Li, M. Peng, K. Zhang, T. Hu, K. Yuan, Y. Chen, *J. Mater. Chem. A* 2021, **9**, 15404-15414.

24 Z. Zhou, X. Zhou, M. Zhang, S. Mu, Q. Liu, Y. Tang, *Small* 2020, **16**, 2003174.

25 B. Xue, J. Xu, R. Xiao, *Chem. Eng. J.* 2023, **454**, 140192.